

AdamNODEs: When Neural ODE Meets Adaptive Moment Estimation

Seunghyeon Cho¹ Sanghyun Hong² Kookjin Lee³ Noseong Park¹

Abstract

Recent work by Xia *et al.* leveraged the continuous-limit of the classical momentum accelerated gradient descent and proposed heavy-ball neural ODEs. While this model offers computational efficiency and high utility over vanilla neural ODEs, this approach often causes the *overshooting* of internal dynamics, leading to unstable training of a model. Prior work addresses this issue by using ad-hoc approaches, *e.g.*, bounding the internal dynamics using specific activation functions, but the resulting models do not satisfy the exact heavy-ball ODE. In this work, we propose adaptive momentum estimation neural ODEs (AdamNODEs) that *adaptively* control the acceleration of the classical momentum-based approach. We find that its adjoint states also satisfy AdamODE and do not require ad-hoc solutions that the prior work employs. In evaluation, we show that AdamNODEs achieve the lowest training loss and efficacy over existing neural ODEs. We also show that AdamNODEs have better training stability than classical momentum-based neural ODEs. This result sheds some light on adapting the techniques proposed in the optimization community to improving the training and inference of neural ODEs further. Our code is available at <https://github.com/pmcsh04/AdamNODE>.

1. Introduction

Neural ordinary differential equations (NODEs) (Chen *et al.*, 2018) are continuous-depth neural networks that perform forward and backward passes by solving an ODE and its adjoint form. NODEs model underlying continuous-time dynamics as a form of ODEs: $\frac{dh}{dt} = \mathbf{f}(\mathbf{h}(t), t; \theta_f)$, where \mathbf{f} is parameterized by a neural network with learnable parameters θ_f . The forward pass is equivalent to solving an initial value problem (IVP) with \mathbf{f} and an initial condition $\mathbf{h}(t_0)$, and the backward pass solves its reverse-mode IVP. By formulating the forward and backward passes into solving an ODE, NODEs improve memory efficiency and scalability of continuous-depth models. (see §2 for the details).

Modeling underlying dynamics using the first-order equation, however, limits the expressivity of a model and often leads to sub-optimal performances. Prior work addresses this issue with diverse approaches. Dupont *et al.* (2019) proposed Augmented Neural ODEs (ANODEs) that solve the ODE on the space with additional dimensions. Norcliffe *et al.* (2020) proposed Second-Order Neural ODEs (SONODEs) and showed that we could generalize the adjoint sensitivity method in the first-order ODEs and solve SONODEs more efficiently. Recent work by Xia *et al.* (2021) leveraged those findings and proposed heavy-ball neural ODEs (HBNODEs) that model the dynamics with the continuous limit of the classical momentum method, suggesting that we may use the knowledge from the optimization literature to improve the training and inference of NODEs further.

In this work, we continue this research direction and characterize the benefit of using adaptive moment estimation in modeling NODEs. Specifically, we ask the question: *How can we model NODEs with adaptive moment estimation, and what*

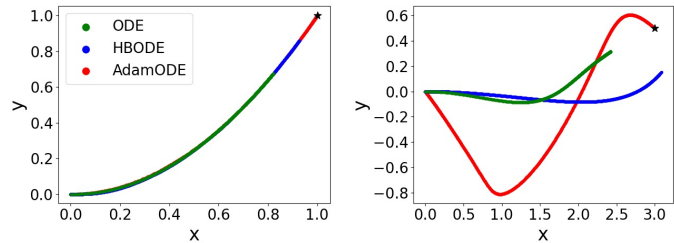


Figure 1. Trajectories computed by solving ODE, HBODE, and AdamODE. We test three different ODE formulations on the Rosenbrock (left) and Beale (right) functions. AdamODE converges to the stationary point (marked as a star) closer and faster than the others.

¹Yonsei University ²Oregon State University ³Arizona State University. Correspondence to: Noseong Park <noseong@yonsei.ac.kr>.

are the benefits over existing NODEs? To motivate, we solve the ODEs with the vanilla, classical momentum (HBODE), and adaptive moment estimation (AdamODE) on the Rosenbrock and Beale functions and contrast the trajectories. In Figure 1, we show that AdamODE converges to the stationary point faster and closer than ODE and HBODE and, thus, is efficient, stable, and accurate. However, it is unknown whether these potential benefits can transfer to NODEs.

Contributions. *First*, we propose AdamNODEs that model the underlying dynamics leveraging the continuous-limit of the adaptive estimates of lower-order moments. Starting from the update rules of Adam optimizer (Kingma & Ba, 2014), we derive the adjoint form of AdamNODEs. This adjoint form is composed of three adjoint equations, making it computationally intractable to solve them directly using the adjoint sensitivity method. *Second*, we solve this form by leveraging the idea of augmenting the solution space, proposed by Dupont et al. (2019), and by projecting each equation to a different dimension. *Third*, we evaluate AdamNODEs on the two image classification tasks and the Silverbox task. In two image classification tasks, AdamNODEs achieve the highest test accuracy per forward or backward NFE compared to the baselines. In the Silverbox task, we show that AdamNODEs can mitigate the overshooting (or the blow-up) problem.

2. Related Work

Continuous-depth neural networks enable flexibility in modeling dynamics and have been studied as a potential alternative to traditional deep feed-forward neural networks (Weinan, 2017; Haber & Ruthotto, 2017; Lu et al., 2018). Chen et al. (2018) addressed the main technical challenge of using continuous-depth networks in practice, *i.e.*, efficient back-propagation through the ODE solver, by using the adjoint sensitivity method. Many continuous-depth models that share the same computational formalism have been proposed, *e.g.*, Neural-Controlled DEs (Kidger et al., 2020) and Neural Stochastic DEs (Liu et al., 2019). Followup work used those models and has shown success in diverse tasks, such as image classification (Zhuang et al., 2020; 2021) or data-driven modeling of physical quantities (Greydanus et al., 2019; Cranmer et al., 2020; Lee et al., 2021). We propose a new continuous-depth network that leverages the adaptive moment estimation.

Modeling ODEs using second-order acceleration. Prior work (Polyak, 1964; Nesterov, 1983; Su et al., 2014; Chen et al., 2014; Wilson et al., 2021) has shown that second-order ODEs with a damping term, such as classical or Nesterov momentum, accelerate the convergence of the first-order ODEs. Xia et al. (2021) leverage this insight and model NODEs with the classical momentum method. The adjoint state of the resulting HBNODEs satisfies an HBNODE, which significantly reduces the number of function evaluations (NFEs) required for forward/backward pass and improves the generalization. However, the classical momentum often causes excessive acceleration, causing the *overshooting* problem (Norcliffe et al., 2020). To address this issue, they propose Generalized HBNODEs (GHBNODEs) that bound the increase of second-order dynamics by using a nonlinear activation, *e.g.*, hardtanh. In contrast, we use adaptive moment estimation and mitigate the overshooting problem while achieving a better test accuracy and computational efficiency than HBNODEs and GHBNODEs.

3. Adaptive Moment Estimation Neural ODEs

3.1. Preliminaries on Heavy-Ball Neural ODEs

NODEs, especially in high accuracy settings, require large computations in training and inference. To mitigate this issue, Xia et al. (2021) have proposed HBNODEs that leverage the concept of the classical momentum. We first review the derivation of HBNODEs from the classical momentum equation (Eq. (1)), where \mathbf{F} is a generic function we optimize:

$$\mathbf{x}^{k+1} = \mathbf{x}^k - s \nabla \mathbf{F}(\mathbf{x}^k) + \beta(\mathbf{x}^k - \mathbf{x}^{k-1}), \quad (1)$$

where $s > 0$ is the step size and $0 \leq \beta \leq 1$ is the momentum scaler. Let $m_k := (x_{k+1} - x_k)/\sqrt{s}$ and $\beta := 1 - \gamma\sqrt{s}$, where $\gamma \geq 0$ is another hyperparameter. Suppose we take the continuous-limit of this form (*i.e.*, $s \rightarrow 0$), Eq. (1) becomes:

$$\frac{\partial \mathbf{x}(t)}{\partial t} = -\mathbf{m}(t), \quad \frac{\partial \mathbf{m}(t)}{\partial t} = -\gamma \mathbf{m}(t) - \nabla \mathbf{F}(\mathbf{x}(t)). \quad (2)$$

Replacing $\mathbf{x}(t)$ with $\mathbf{h}(t)$ and parameterizing $-\nabla \mathbf{F}$ as a neural network $\mathbf{f}(\mathbf{h}(t), t; \theta_f)$ yields HBNODEs:

$$\frac{\partial \mathbf{h}(t)}{\partial t} = -\mathbf{m}(t), \quad \frac{\partial \mathbf{m}(t)}{\partial t} = -\gamma \mathbf{m}(t) + \mathbf{f}(\mathbf{h}(t), t; \theta_f), \quad (3)$$

that can be rewritten with initial position $\mathbf{h}(t_0)$ and momentum $\mathbf{m}(t_0) := d\mathbf{h}/dt(t_0)$ as follows:

$$\frac{\partial^2 \mathbf{h}(t)}{\partial t^2} + \gamma \frac{\partial \mathbf{h}(t)}{\partial t} = \mathbf{f}(\mathbf{h}(t), t; \theta_f). \quad (4)$$

HBNODE (Eq. (4)) requires fewer computations in solving and is well-structured; thus, it also alleviates vanishing gradients. However, the momentum acceleration often increases too fast, and this leads to the blow-up issue.

3.2. AdamNODEs: Adaptive Moment Estimation NODEs

Adam (Kingma & Ba, 2014) is an optimization method that combines the existing momentum and RMSProp methods. It gives inertia to the progressing speed and has an adaptive learning rate according to the amount of change in the curved surface of the recent path. Following the procedure similar to §3.1, we derive AdamNODEs from the update rule of Adam:

$$\begin{cases} \mathbf{x}_{k+1} &= \mathbf{x}_k - s\mathbf{m}_k/\sqrt{\mathbf{v}_k + \epsilon}, \\ \mathbf{m}_{k+1} &= \alpha\mathbf{m}_k + (1 - \alpha)\nabla\mathbf{F}(\mathbf{x}_{k+1}), \\ \mathbf{v}_{k+1} &= \beta\mathbf{v}_k + (1 - \beta)\nabla\mathbf{F}(\mathbf{x}_{k+1})^2. \end{cases} \quad (5)$$

where \mathbf{m} denotes the momentum term and \mathbf{v} denotes the adaptive step term. Converting this rule into a form of ODE gives:

$$\begin{cases} \frac{\partial\mathbf{x}(t)}{\partial t} &= -\mathbf{m}(t)/\sqrt{\mathbf{v}(t) + \epsilon}, \\ \frac{\partial\mathbf{m}(t)}{\partial t} &= (1 - \alpha)(\nabla\mathbf{F}(\mathbf{x}(t)) - \mathbf{m}(t)), \\ \frac{\partial\mathbf{v}(t)}{\partial t} &= (1 - \beta)(\nabla\mathbf{F}(\mathbf{x}(t))^2 - \mathbf{v}(t)). \end{cases} \quad (6)$$

As has been done in deriving HBNODEs (Eq. (3)), replacing $\mathbf{x}(t)$ with $\mathbf{h}(t)$ and parameterizing $-\nabla\mathbf{F}$ as a neural network $\mathbf{f}(\mathbf{h}(t), t, \theta_f)$ yields AdamNODEs such that:

$$\begin{cases} \frac{\partial\mathbf{h}(t)}{\partial t} &= -\mathbf{m}(t)/\sqrt{\mathbf{v}(t) + \epsilon}, \\ \frac{\partial\mathbf{m}(t)}{\partial t} &= (1 - \alpha)(-\mathbf{f}(\mathbf{h}(t), t; \theta_f) - \mathbf{m}(t)), \\ \frac{\partial\mathbf{v}(t)}{\partial t} &= (1 - \beta)(\mathbf{f}(\mathbf{h}(t), t; \theta_f)^2 - \mathbf{v}(t)). \end{cases} \quad (7)$$

3.3. Adjoint Equation of AdamNODEs

If we denote the loss, which measures the discrepancy between the prediction $\mathbf{h}(t_1)$ and the ground truth as \mathbf{L} , the backward pass to update the model parameters θ_f can be represented as systems of ODEs:

$$\frac{d\mathbf{L}(\mathbf{h}(t_1))}{dt} = \int_{t_0}^{t_1} \mathbf{a}(t) \frac{\partial\mathbf{f}(\mathbf{h}(t), t; \theta_f)}{\partial\theta} dt, \quad (8)$$

$$\frac{d\mathbf{a}(t)}{dt} = -\mathbf{a}(t) \frac{\partial\mathbf{f}(\mathbf{h}(t), t; \theta_f)}{\partial\mathbf{h}}, \quad (9)$$

where $\mathbf{a}(t) = \frac{\partial\mathbf{L}}{\partial\mathbf{h}(t)}$ is the adjoint state. Satisfying the adjoint state is important in reducing the computations as it allows us to compute the backward pass by solving the reverse-mode IVP from the final state towards the initial state. The adjoint equations of AdamNODEs are written as follows (we skip the full derivation process due to the space limitation):

$$\begin{cases} \frac{\partial\mathbf{a}_h(t)}{\partial t} &= -\left(-\frac{\partial\mathbf{f}(\mathbf{h}(t), t; \theta_f)}{\partial\mathbf{h}}\mathbf{a}_m(t) + \frac{\partial\mathbf{f}(\mathbf{h}(t), t; \theta_f)}{\partial\mathbf{h}}\mathbf{a}_v(t)\right), \\ \frac{\partial\mathbf{a}_m(t)}{\partial t} &= -\left(-\frac{1}{\sqrt{v(t)+\epsilon}}\mathbf{a}_h(t) - (1 - \alpha)\mathbf{a}_m(t)\right), \\ \frac{\partial\mathbf{a}_v(t)}{\partial t} &= -\left(\frac{m}{2(v(t)+\epsilon)\sqrt{v(t)+\epsilon}}\mathbf{a}_h(t) - (1 - \beta)\mathbf{a}_v(t)\right). \end{cases} \quad (10)$$

We solve the adjoint equations using the computationally efficient technique proposed by Dupont et al. (2019). Detailed proofs can be found in Appendix A.

4. Experimental Results

We now evaluate the accuracy, efficiency, and stability of AdamNODEs using the following metrics:

Metrics. We use the *classification accuracy* (henceforth, we call *accuracy*) on the train-set to measure the generalization performance. To measure the computational efficiency of AdamNODEs, we define the test accuracy per the number of function evaluations (NFE), *efficacy* in short, in the forward and backward passes. Efficacy shows the performance advantage

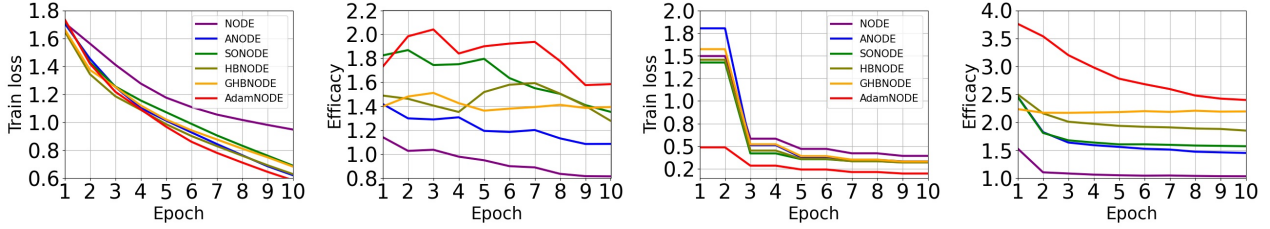


Figure 2. **Contrasting AdamNODEs and the five baseline models trained on CIFAR-10 and MNIST.** The left two figures show our CIFAR10 results, and the results from MNIST are shown in the right two figures. We show the training loss and efficacy (*i.e.*, the accuracy per NFE) over 10 epochs. In both CIFAR-10 and MNIST, AdamNODEs achieve the lowest training loss and the highest efficacy. We also compare the training time and the memory efficiency of AdamNODEs with the baseline models in Appendix B and C, respectively.

of a model per the unit of computations (NFE). Following the prior work (Xia et al., 2021), we measure the stability of AdamNODEs by computing the ℓ_2 -norm of $\mathbf{h}(t)$ over time. The smaller the $\|\mathbf{h}(t)\|_{\ell_2}$ is, the more stable a model is.

Datasets and baselines. We consider five existing NODEs as our baselines: NODE (Chen et al., 2018), ANODE (Dupont et al., 2019), SONODE (Norcliffe et al., 2020), HBNODE (Xia et al., 2021), and GHBNODE (Xia et al., 2021). To compare the accuracy and efficacy, we train them on two image classification benchmarks: MNIST (LeCun et al., 2010) and CIFAR-10 (Krizhevsky et al., 2009). We also experiment on the Silverbox tasks (Norcliffe et al., 2020) to compare the stability of the training process. In Silverbox, the rapid increase of $\|\mathbf{h}(t)\|_{\ell_2}$ leads to the finite-time *blow-up* and makes it difficult to train models. For a fair comparison, we made the number of parameters of all our models close to each other.

To train those models, we use the Adam optimizer (Kingma & Ba, 2014). In CIFAR10, we set the learning rate to 0.001 and batch size to 64. We use the learning rate of 0.0001 and the batch size of 32 in MNIST. We use Dormand-Prince-45 as the numerical ODE solver. For HBNODE and GHBNODE, we set the damping parameter γ to $\text{sigmoid}(\theta)$, where θ is a trainable and initialized to -3. We use a 3-layer convolutional neural network to parameterize $f(\mathbf{h}(t), t; \theta_f)$. We use Python v3.7 and TorchDiffEq¹. We run all our experiments on a machine equipped with 3 Nvidia RTX A6000 GPUs.

Image classification results. Figure 2 illustrates our MNIST and CIFAR-10 results. We first highlight that AdamNODEs achieve the lower training loss and higher efficacy over the baseline models. In particular, the efficacy of AdamNODEs is 20% higher than the momentum-based HBNODEs and 80% higher than the vanilla NODEs. We observe the consistent results in MNIST. AdamNODE’s accuracy is 0.95% point higher than the best existing model — we omit the accuracy table for space reasons.

The Silverbox task results. We also show that AdamNODE stabilizes the training process. The results are shown in Figure 3. We train the five baseline models and AdamNODE on the Silverbox task and plot the changes in $\|\mathbf{h}(t)\|_{\ell_2}$ as t increases. We find that, at $t=64$, AdamNODE has $10^{18} \times$ smaller $\|\mathbf{h}(t)\|_{\ell_2}$ value than that of HBNODE. We also show that, compared to the $\|\mathbf{h}(t)\|_{\ell_2}$ value of NODE at $t=64$, AdamNODE has $10^{12} \times$ smaller one. GHBNODE shows the $\|\mathbf{h}(t)\|_{\ell_2}$ value similar to that of AdamNODE. Note that AdamNODE achieves a similar stability without using any bounded activation function that requires for GHBNODEs.

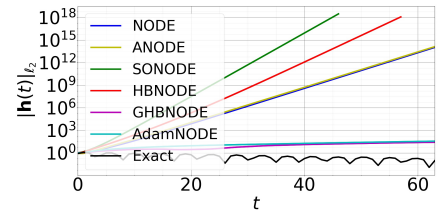


Figure 3. **Contrasting $\mathbf{h}(t)$ for six models.** $\|\mathbf{h}(t)\|_{\ell_2}$ in HBNODE increases much faster than AdamNODEs as t increases.

5. Conclusions and Future Work

This work proposes AdamNODEs to improve the performance, efficiency, and stability of the training and inference of NODEs further. We show that AdamNODEs achieve the lowest training loss and improve the training and inference efficacy by 20–80% over existing baseline NODEs. We also demonstrate that AdamNODEs mitigate the blow-up issue without taking the ad-hoc solutions the classical momentum-based neural ODEs (*e.g.*, HBNODEs or GHBNODEs) use.

What’s Next? The result suggests that future work is needed for adapting advanced algorithms proposed in the optimization community to NODEs. As shown in Figures 2 and 3, we may achieve a better utility in conjunction with the ease of training. One can also explore the use of adaptive moment estimation in generative modeling or normalizing flows.

¹<https://github.com/rtqichen/torchdiffeq>

References

- Chen, R. T., Rubanova, Y., Bettencourt, J., and Duvenaud, D. K. Neural ordinary differential equations. *Advances in neural information processing systems*, 31, 2018.
- Chen, T., Fox, E., and Guestrin, C. Stochastic gradient hamiltonian monte carlo. In *International conference on machine learning*, pp. 1683–1691. PMLR, 2014.
- Cranmer, M., Greydanus, S., Hoyer, S., Battaglia, P., Spergel, D., and Ho, S. Lagrangian neural networks. In *ICLR 2020 Workshop*, 2020.
- Dupont, E., Doucet, A., and Teh, Y. W. Augmented neural odes. *Advances in Neural Information Processing Systems*, 32, 2019.
- Greydanus, S., Dzamba, M., and Yosinski, J. Hamiltonian neural networks. *Advances in Neural Information Processing Systems*, 32:15379–15389, 2019.
- Haber, E. and Ruthotto, L. Stable architectures for deep neural networks. *Inverse problems*, 34(1):014004, 2017.
- Kidger, P., Morrill, J., Foster, J., and Lyons, T. Neural controlled differential equations for irregular time series. *Advances in Neural Information Processing Systems*, 33:6696–6707, 2020.
- Kingma, D. P. and Ba, J. Adam: A method for stochastic optimization. *arXiv preprint arXiv:1412.6980*, 2014.
- Krizhevsky, A., Hinton, G., et al. Learning multiple layers of features from tiny images. 2009.
- Langley, P. Crafting papers on machine learning. In Langley, P. (ed.), *Proceedings of the 17th International Conference on Machine Learning (ICML 2000)*, pp. 1207–1216, Stanford, CA, 2000. Morgan Kaufmann.
- LeCun, Y., Cortes, C., and Burges, C. Mnist handwritten digit database. *ATT Labs [Online]*. Available: <http://yann.lecun.com/exdb/mnist>, 2, 2010.
- Lee, K., Trask, N., and Stinis, P. Machine learning structure preserving brackets for forecasting irreversible processes. In *Thirty-Fifth Conference on Neural Information Processing Systems*, 2021.
- Liu, X., Xiao, T., Si, S., Cao, Q., Kumar, S., and Hsieh, C.-J. Neural sde: Stabilizing neural ode networks with stochastic noise. *arXiv preprint arXiv:1906.02355*, 2019.
- Lu, Y., Zhong, A., Li, Q., and Dong, B. Beyond finite layer neural networks: Bridging deep architectures and numerical differential equations. In *International Conference on Machine Learning*, pp. 3276–3285. PMLR, 2018.
- Nesterov, Y. A method for unconstrained convex minimization problem with the rate of convergence $O(1/k^2)$. In *Doklady an ussr*, volume 269, pp. 543–547, 1983.
- Norcliffe, A., Bodnar, C., Day, B., Simidjievski, N., and Liò, P. On second order behaviour in augmented neural odes. *Advances in Neural Information Processing Systems*, 33:5911–5921, 2020.
- Polyak, B. T. Some methods of speeding up the convergence of iteration methods. *Ussr computational mathematics and mathematical physics*, 4(5):1–17, 1964.
- Su, W., Boyd, S., and Candes, E. A differential equation for modeling nesterov’s accelerated gradient method: theory and insights. *Advances in neural information processing systems*, 27, 2014.
- Weinan, E. A proposal on machine learning via dynamical systems. *Communications in Mathematics and Statistics*, 1(5): 1–11, 2017.
- Wilson, A. C., Recht, B., and Jordan, M. I. A lyapunov analysis of accelerated methods in optimization. *Journal of Machine Learning Research*, 22(113):1–34, 2021.
- Xia, H., Suliafu, V., Ji, H., Nguyen, T., Bertozzi, A., Osher, S., and Wang, B. Heavy ball neural ordinary differential equations. *Advances in Neural Information Processing Systems*, 34, 2021.

Zhuang, J., Dvornek, N., Li, X., Tatikonda, S., Papademetris, X., and Duncan, J. Adaptive checkpoint adjoint method for gradient estimation in neural ode. In *International Conference on Machine Learning*, pp. 11639–11649. PMLR, 2020.

Zhuang, J., Dvornek, N. C., Tatikonda, S., and Duncan, J. S. Mali: A memory efficient and reverse accurate integrator for neural odes. *arXiv preprint arXiv:2102.04668*, 2021.

A. The Adjoint Equation for AdamNODEs

We describe the details of deriving the adjoint equations for AdamNODEs as follows:

$$\begin{cases} \frac{\partial \mathbf{h}(t)}{\partial t} &= -\mathbf{m}(t)/\sqrt{\mathbf{v}(t)+\epsilon}, \\ \frac{\partial \mathbf{m}(t)}{\partial t} &= (1-\alpha)(-\mathbf{f}(\mathbf{h}(t), t; \theta_f) - \mathbf{m}(t)), \\ \frac{\partial \mathbf{v}(t)}{\partial t} &= (1-\beta)(\mathbf{f}(\mathbf{h}(t), t; \theta_f)^2 - \mathbf{v}(t)). \end{cases} \quad (11)$$

Denote that the initial state $t=t_0$ and final state $t=T$ as

$$\begin{bmatrix} \mathbf{h} \\ \mathbf{m} \\ \mathbf{v} \end{bmatrix} (t_0) = \begin{bmatrix} \mathbf{h}_{t_0} \\ \mathbf{m}_{t_0} \\ \mathbf{v}_{t_0} \end{bmatrix}, \quad \begin{bmatrix} \mathbf{h} \\ \mathbf{m} \\ \mathbf{v} \end{bmatrix} (T) = \begin{bmatrix} \mathbf{h}_T \\ \mathbf{m}_T \\ \mathbf{v}_T \end{bmatrix} = z. \quad (12)$$

Using the proof from Xia et al. (2021), we have the adjoint equations as the following form:

$$\frac{\partial \mathbf{A}(t)}{\partial t} = -\mathbf{A}(t) \begin{bmatrix} 0 & \frac{-1}{\sqrt{v(t)+\epsilon}} & \frac{m}{2(v(t)+\epsilon)\sqrt{v(t)+\epsilon}} \\ -\frac{\partial \mathbf{f}(\mathbf{h}(t), t; \theta_f)}{\partial \mathbf{h}} & (1-\alpha)I & 0 \\ \frac{\partial \mathbf{f}(\mathbf{h}(t), t; \theta_f)}{\partial \mathbf{h}} & 0 & (1-\beta)I \end{bmatrix}, \quad \mathbf{A}(T) = -\mathbf{I}, \quad \mathbf{a}(t) = \frac{\partial L}{\partial z} \mathbf{A}(t). \quad (13)$$

Suppose $\mathbf{a} = [\mathbf{a}_h \ \mathbf{a}_m \ \mathbf{a}_v]$, the above equations become:

$$\frac{\partial [\mathbf{a}_h \ \mathbf{a}_m \ \mathbf{a}_v]}{\partial t} = -[\mathbf{a}_h \ \mathbf{a}_m \ \mathbf{a}_v] \begin{bmatrix} 0 & \frac{-1}{\sqrt{v(t)+\epsilon}} & \frac{m}{2(v(t)+\epsilon)\sqrt{v(t)+\epsilon}} \\ -\frac{\partial \mathbf{f}(\mathbf{h}(t), t; \theta_f)}{\partial \mathbf{h}} & (1-\alpha)I & 0 \\ \frac{\partial \mathbf{f}(\mathbf{h}(t), t; \theta_f)}{\partial \mathbf{h}} & 0 & (1-\beta)I \end{bmatrix}, \quad (14)$$

We now simplify Eq. 14 as follows:

$$\begin{cases} \frac{\partial \mathbf{a}_h(t)}{\partial t} &= -\left(-\frac{\partial \mathbf{f}(\mathbf{h}(t), t; \theta_f)}{\partial \mathbf{h}} \mathbf{a}_m(t) + \frac{\partial \mathbf{f}(\mathbf{h}(t), t; \theta_f)}{\partial \mathbf{h}} \mathbf{a}_v(t)\right), \\ \frac{\partial \mathbf{a}_m(t)}{\partial t} &= -\left(-\frac{1}{\sqrt{v(t)+\epsilon}} \mathbf{a}_h(t) - (1-\alpha) \mathbf{a}_m(t)\right), \\ \frac{\partial \mathbf{a}_v(t)}{\partial t} &= -\left(\frac{m}{2(v(t)+\epsilon)\sqrt{v(t)+\epsilon}} \mathbf{a}_h(t) - (1-\beta) \mathbf{a}_v(t)\right). \end{cases} \quad (15)$$

B. Training Time

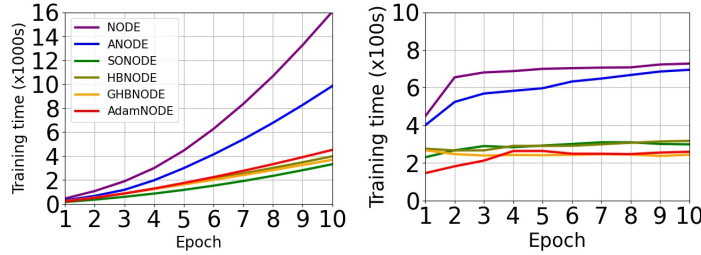


Figure 4. **Comparison of the training time for different models.** We compare the training time of five baseline NODEs with AdamNODEs. We measure the wall-time difference between the start and the end of training. We show the CIFAR10 (left) and MNIST (right) results. We find that AdamNODEs achieve the training time similar to the momentum-based HBNODEs and GHBNODEs.

Here, we examine whether AdamNODEs increase the training time of the momentum-based models, such as HBNODEs or GHBNODEs. Due to the adaptive moment estimation, we hypothesize that AdamNODEs may require a longer training time than the momentum-based NODEs. Hence, we compare the training time for the NODEs we use in our experiments. The results are shown in Figure 4. We observe that AdamNODEs do not increase the training time of HBNODEs or GHBNODEs. In both CIFAR10 and MNIST, AdamNODEs' training time is the same as that of the momentum-based NODEs.

C. Memory Efficiency

	NODE	ANODE	SONODE	HBNODE	GHBNODE	AdamNODE
CIFAR10	2469 MiB	2485 MiB	2863 MiB	2891 MiB	2889 MiB	3531 MiB

Table 1. Comparison of memory efficiency for different models. We compare the memory efficiency of five baseline NODEs with our AdamNODEs. We measure the memory footprints in MiB. We find that AdamNODEs require slightly more memory than the baselines.

We compare the memory footprints of AdamNODEs with five baselines. Table 1 shows our results. We confirmed that the memory footprints of NODEs and ANODEs are the same. The memory footprint is larger in SONODEs and (G)HBNODEs than ANODEs as there are additional variables (e.g., velocity). AdamNODEs show the increased memory footprint as there are more additional variables (e.g., velocity or variables for adaptive moment estimation).